# Step-up DC-DC Converter Supplied by a Thermoelectric Generator for IoT Applications

José Almeida
*Academia Militar*
Lisboa, Portugal
josesalmeida@tecnico.ulisboa.pt

Pedro Santos
*Academia Militar*
Lisboa, Portugal
pedro.santos@lx.it.pt

João Vaz
*Instituto Superior Técnico*
Lisboa, Portugal
joaovaz@tecnico.ulisboa.pt

***Abstract*—Autonomous and portable electronic circuits are typically powered by a battery. These batteries are bulky and have a limited life span. Thus, there is a need to study an alternative to replace batteries with low-cost energy harvesting sources. These sources are capable of powering several applications like portable and wearable electronics and remote sensors.**

**This dissertation's main objective is to design and prototype a DC-DC converter to step-up the low voltage of a small low-power thermoelectric generator, with input voltages of hundreds of mV, to attain a regulated output voltage of 1.2V. After the theoretical analysis and simulation of the converter, several possibilities for sizing the converter are experimentally tested and compared with each other, to be implemented only with components off-the-shelf (COTS).**

**In order to be a standalone system, it was also necessary to design an oscillator to drive the MOSFET with a switching frequency of a few MHz. We introduced a super-capacitor in the circuit to better function the TEG as a power supply.**

**Finally, with the inclusion of a Low-dropout regulator and the experimental validation of the final prototype, it was possible to observe a regulated voltage at the output of 1.2 V.**

***Index Terms*—DC-DC converter, energy harvesting, thermoelectric generator.**

## I. Introduction

The idea of IoT (Internet of Things), where devices with embedded electronics, sensors, actuators, and software are connected and interact over the internet, has gained wide attention [Nozariasbmarz et al., 2020]. Wearable technology is also the target of growing interest for personal health monitoring and the use of various electronic sensors. A combination of IoT and wearables can improve quality of life by reducing the cost of [Liu and Zhao, 2020] healthcare, as well as monitoring daily training and performance.

Thermoelectric generators, TEG, together with photovoltaic cells, are the most promising *Energy Harvesting* (EH) sources for very low voltage and low power applications. The output power and voltage available in the TEG generally ranges from $10muW$ to $10mW$ and from 50 to 600 $mV$ respectively. The actual values depend on the differences in temperature and size of the TEG [Bandyopadhyay and Chandrakasan, 2012]. To power a battery or IoT device, it is necessary to convert the output voltage of the TEG, to a standard output voltage (1.2V, 2.4V, 3.3V and 4.6V) [Sze et al., 2008] [Ammar et al., 2020].

## II. State-of-art

Table I presents topologies of converters proposed in the scope of energy harvesting. The parameters under analysis for comparing the different typologies are the input and output voltage, the occupied area, the switching frequency, the efficiency, the presence of external coils, the manufacturing process, the architecture of the step-up DC-DC converter, and the circuit-specific power supply.

The works in Table I are from the step-up DC-DC converter. All the works present variations to improve the performance of the dimensioned converter, raising the output voltage as much as possible and allowing very low voltage inputs. Some systems require an external source for the start-up, like a piezoelectric [Romani et al., 2015] or a super-capacitor [Carlson et al., 2010]. Throughout the analysis, we noticed that the developed systems often featured Maximum Power Point Tracking, control circuits, and the use of transformers as a solution to startup the circuit [Im et al., 2012] e [Chandrarathna and Lee, 2019]. The circuit presented in [Bose et al., 2019] and [Radin et al., 2019]is based on a charge pump topology.

## III. TEG

The thermoelectric generator (TEG) is a device that produces electrical energy from the difference in temperature applied between two surfaces. This technology was discovered by Thomas Johann Seebeck in 1821 [Gould et al., 2008]. According to Seebeck, it is possible to obtain an electrical potential difference by applying a temperature difference to two types of materials. As a result, this phenomenon is known as the *Seebeck* effect. In Figure 1 we observe the experimental data when we apply a temperature difference to the TEG through a heating plate. Initially, the temperature $T_c$ and $T_h$ is 25ºC. Then we applied the heating plate to the TEG hot zone and generated a voltage in the TEG terminals due to the temperature difference that at 20 seconds was $T_h$=230ºC. We measured this value with a digital thermometer ICEL MD 5770, where we observed the various values on the surface of the hot side of the TEG over 20 seconds of heating.

It is important to highlight that, in this case study, we only used one TEG module. If several of these modules are put in series, obtaining about 0.5V with a smaller temperature difference is possible. Using five modules equal to the TEG

TABLE I
COMPARISON OF DIFFERENT VOLTAGE BOOSTING DC-DC CONVERTER TOPOLOGIES USED IN ENERGY HARVESTING.

| Parameters | Articles | | | | | |
|---|---|---|---|---|---|---|
| | [Carlson et al., 2010] | [Im et al., 2012] | [Romani et al., 2015] | [Chandrarathna and Lee, 2019] | [Bose et al., 2019] | [Radin et al., 2019] |
| Year | 2010 | 2012 | 2015 | 2019 | 2019 | 2019 |
| Vin (mV) | 20 | 40 | 16 | 20 | 57 | 11 |
| Vout (V) | 1 | 2 | 1,32 | 1.2 | - | - |
| Area (mm2) | 4,5 | - | - | 0,46 | 0,96 | 0,93 |
| Frequency | 0,22 - 3,1 MHz | 439 kHz | 1 kHz | 80 kHz | 25 KhZ | 3,9 MHz |
| Efficiency | 75% | 61% | 40% | 81,5 % | - | 85% @140 mV |
| L (uH) | 4,7 | - | 37 | 100 | 220 | - |
| Process | CMOS 130nm | CMOS 130nm | - | CMOS 180nm | CMOS 180nm | CMOS 130 nm |
| Architecture | Inductive Boost | Transformer | Inductive Boost | Transformer | Inductive Boost | Inductive Boost |
| Source | TEG | TEG | Piezoelectric | TEG | TEG | TEG |

used in this Thesis, with a temperature difference of 35ºC, it is possible to obtain the desired 0.5V, occupying a reduced area of 6.3$cm^2$.

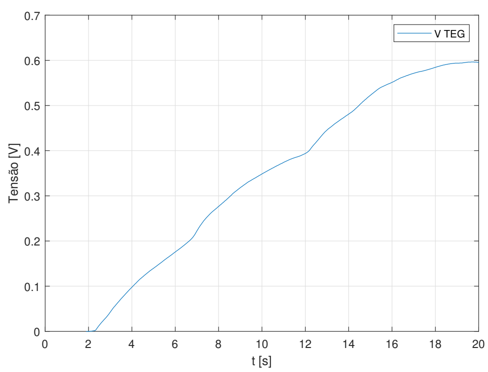


Fig. 1. Variation of TEG Voltage with time, while heating TEG, with initial temperature of 25ºC and final temperature in the hot side of 230ºC.

## IV. EXPERIMENTAL REALISATION

### A. Step-up DC-DC Converter

Initially, the dimensioned circuit was assembled on a test board, according to the schematic present in the Figure 2, with L = 150 uH, C = 4.7 nF and $R_L$ = 100 kΩ. In Figure 3, one can observe the output of the DC-DC voltage step-up converter as a function of time for the initial conditions considered. An output of 2.2 V can be observed in the converter, for an input voltage of 0.5V, with an input signal at the *gate* of the MOSFET varying between 0 V and 0.5 V, with D = 50% and $f_C$ = 1 MHz.

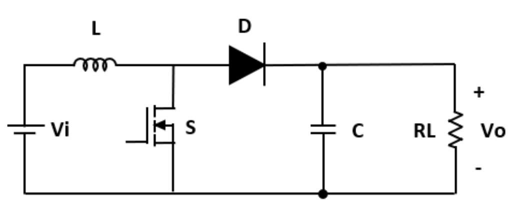


Fig. 2. Schematic of the Step-up DC-DC Converter.

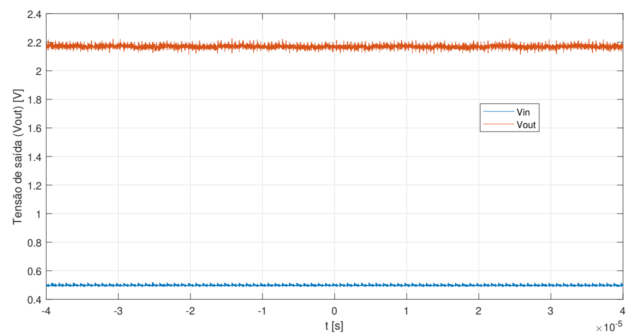


Fig. 3. Time diagram of the output voltage of the Step-up DC-DC Converter (orange) for Vin = 0.5 V (blue), $f_c$ = 1 MHz, D = 50%.

### B. Colpitts LC Oscillator

The Oscillator was assembled on a test board, according to the schemtic present in Figure 4, the values used in the feedback loop of the oscillator were, L = 470 uH, R = 1.2 kΩ, $C_1$ = 10 pF, $C_2$ = 47 pF. Figure 5 shows the waveform of the oscillator assembled on the test board, highlighting the fact that it has an oscillation frequency of 1.04 MHz, which is very close to the intended specifications for a cycle factor of approximately 50%.

With the oscillator working for the desired 0.5 V input voltage, it is possible to have a circuit that only depends on the input voltage and does not need an external oscillator for its operation, which is fundamental for the circuit to be autonomous.

## V. REALISATION OF THE FINAL PROTOTYPE

Figure 6 shows the final prototypes of the boost converter with and without a super-capacitor. As we can see, the circuit has a low dimension (4.8 $cm^2$), and in the case of not using the super-condenser, we can reduce the size to half. The left Figure 6, shows a super-capacitor, two coils, a resistor, three capacitors, a Low-Dropout, a Schottky diode, and the integrated circuit containing two transistors. The sum of all the components is equal to nine, which is a low number of components, considering that it meets the objectives of the dissertation.

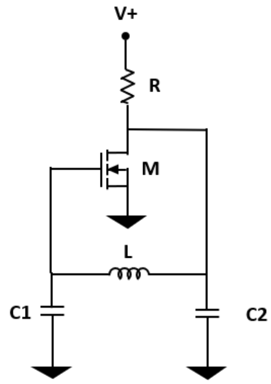


Fig. 4. Schematic of Colpitts LC oscillator.

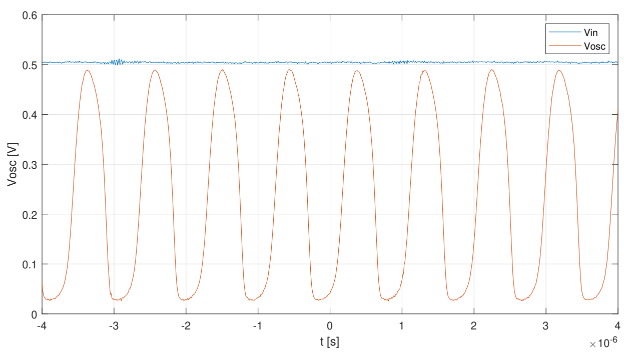


Fig. 5. Waveform resulting from the experimental setup, on the test board, of Colpitts LC oscillator for an input voltage of 0.5 V.

In Figure 7 the timing diagram is presented for the two final prototype cases, with and without super-capacitor. The circuit is fed by an ideal input voltage of 0.5V, with $R_L = 100\text{k}\Omega$ and observing the voltage at the boost converter's output and the LDO output for both cases. Note that we observe a much higher value in the boost converter with the super-capacitor than that observed without the super-capacitor. This difference is explained by the fact that the super-capacitor acts as a battery and allows the current in the circuit to be higher. It is also important to verify that the voltage regulator is working as foreseen in the specifications, with a voltage regulated at 1.2 V.

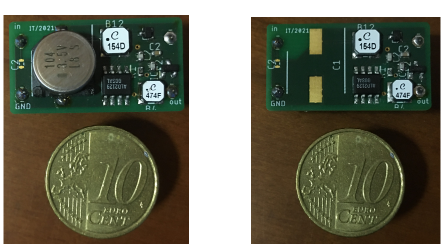

Fig. 6. Final prototype of the *boost* converter with (left) and without (right) super-capacitor.

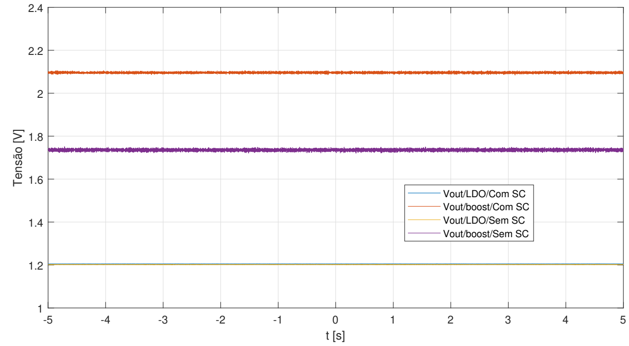


Fig. 7. Time diagram for the two final prototype cases, with and without super-capacitor. Being the circuit fed by an ideal input voltage of 0.5V, with $R_L$ = 100k$\Omega$ and observing the voltage at the output of the converter boost and at the LDO output for both cases.

### *A. Analysis of the influence of the load resistance in the final prototype*

We can observe in Figure 8 that for higher resistances, the voltage at the output of the converter boost is higher, as expected. However, zooming in near 1.2 V, we see that one output voltage is not regulated. It is the one corresponding to the load resistance of 22 k$\Omega$, which can be explained by the fact that the output voltage of the corresponding converter boost is below the 1.4 V, indicated in the datasheet of the LDO.

This analysis shows that the load resistance must be higher than 22 k$\Omega$, being this one of the limit conditions.

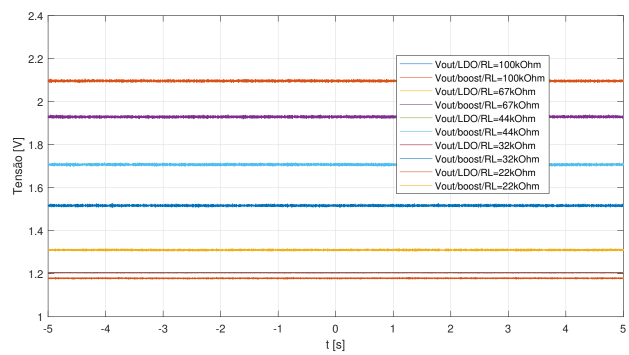


Fig. 8. Time diagram for the analysis of the influence of the load resistance $R_L$ in the final prototype with super-capacitor. Being the circuit fed by an ideal input voltage of 0.5V and observing the voltage at the output of the converter *boost* and the LDO.

### *B. Analysis of the influence of the input voltage on the final prototype*

As expected, the higher the input voltage, the higher the output voltage in the boost. For values of output voltage in the boost lower than 1.4 V, the output voltage in the LDO is no longer regulated at 1.2 V, as we can see in Figure 9. We observe that for input voltage values of 405 mV and 415 mV, the boost converter works. However, the output voltage of the boost converter is 1.24 V and 1.3 V, respectively. Thus the output at the voltage regulator will not be controlled, as the LDO requires a minimum input of 1.4 V. This is another boundary condition in our prototype. In order to regulate the output voltage

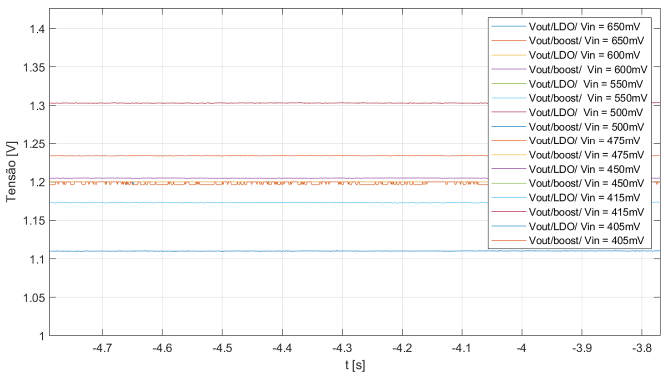


Fig. 9. Time diagram for the analysis of the influence of the input voltage on the output voltage of the LDO.

### *C. Analysis of the final prototype having as input voltage the TEG terminals*

Figure 10 shows the output voltage of the boost converter and the output voltage of the LDO when the voltage at the TEG terminals powers the circuit. Initially, we applied a temperature difference to the TEG until about twenty seconds. Then the TEG is disconnected from the board by a push button. This push button was a solution applied on the workbench so that the TEG did not remove power from the circuit. After the TEG is switched off, the output voltage on the LDO remains regulated for another fifteen seconds, which is a sufficient time span for numerous electronic system applications. In Figure 11 unlike the previous case, we do not have the super-capacitor in the circuit. Therefore, although everything else is the same, at the time when we no longer apply a temperature difference to the TEG (17 seconds), the output voltage of the *boost* drops abruptly. Consequently, the output voltage at the LDO only remains constant for another two seconds.

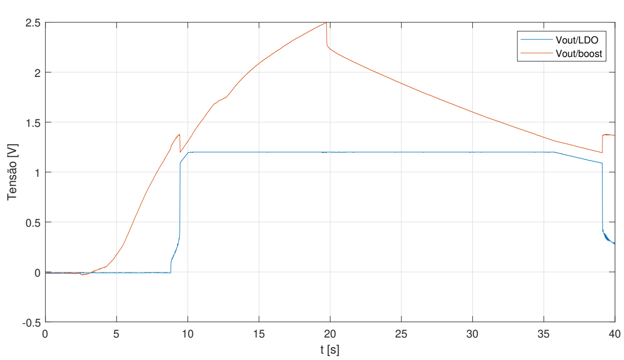


Fig. 10. Time diagram for the analysis of the influence of the super-capacitor in the final prototype with $R_L$ = 100 k$\Omega$, when the input voltage is given by the TEG. Observing the voltage at the output of the *boost* converter and the LDO.

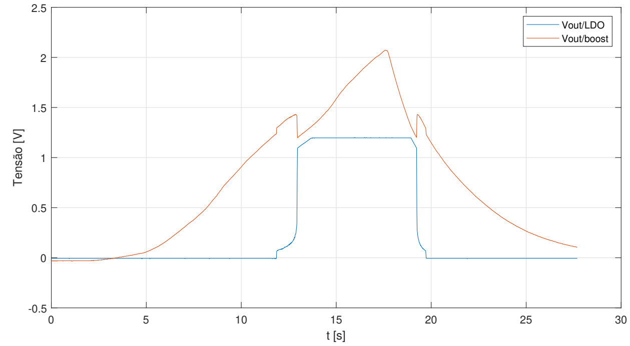


Fig. 11. Time diagram for the analysis of the influence without super-capacitor in the final prototype with $R_L$ = 100 k$\Omega$, when the input voltage is given by the TEG. Observing the voltage at the output of the *boost* converter and the LDO.

## VI. Conclusion

Initially, we researched the operation of the TEG, which was fundamental to understanding the operation of the TEG. With the help of the available tools, it was possible to simulate the TEG, which was a good starting point to know with which input voltages we could work.

Subsequently, we designed a DC-DC voltage step-up converter, with the main characteristics of having an input voltage in accordance with the TEG, having a switching frequency of 1 MHz and a cycle factor of 50% and an output voltage of about 1.2 V.

After the necessary adjustments for the experimental part and with the step-up DC-DC converter working, it was necessary to design an oscillator to make the circuit standalone. This oscillator should meet the assumption previously defined regarding the input voltage that could not be higher than the voltage obtained at the TEG terminals, the switching frequency of 1 MHz, and the cycle factor of 50%.

After sizing the oscillator and with the circuit operating autonomously, the need arose to have a regulated output. For this, we used the voltage regulator - LDO, capable of regulating a variable input voltage between 1.4 V and 5.5 V at a fixed voltage of 1.2V. We also experimented using a super-capacitor at the input of the *boost* converter, which allowed a higher voltage output and also the functioning of the prototype regulating the voltage during more time than the time in which we apply a temperature difference in the TEG.

Finally, and with all the knowledge acquired throughout the dissertation work comes the experimental realization of the final prototype. We analyzed to understand the limits of operation and verified the correct operation with the TEG.

## Acknowledgment


A special thank to the Instituto de Telecomunicações for funding my dissertation, as well as for providing the laboratory space and material necessary for the experimental realization of this dissertation.

# REFERENCES


[Ammar et al., 2020] Ammar, M. B., Sahnoun, S., Fakhfakh, A., and Kanoun, O. (2020). Design of a dc-dc boost converter of hybrid energy harvester for iot devices. In *2020 IEEE 6th World Forum on Internet of Things (WF-IoT)*, pages 1–4. IEEE.

[Bandyopadhyay and Chandrakasan, 2012] Bandyopadhyay, S. and Chandrakasan, A. P. (2012). Platform architecture for solar, thermal, and vibration energy combining with mppt and single inductor. *IEEE Journal of Solid-State Circuits*, 47(9):2199–2215.

[Bose et al., 2019] Bose, S., Anand, T., and Johnston, M. L. (2019). Integrated cold start of a boost converter at 57 mv using cross-coupled complementary charge pumps and ultra-low-voltage ring oscillator. *IEEE journal of solid-state circuits*, 54(10):2867–2878.

[Carlson et al., 2010] Carlson, E. J., Strunz, K., and Otis, B. P. (2010). A 20 mv input boost converter with efficient digital control for thermoelectric energy harvesting. *IEEE Journal of Solid-State Circuits*, 45(4):741–750.

[Chandrarathna and Lee, 2019] Chandrarathna, S. C. and Lee, J.-W. (2019). A dual-stage boost converter using two-dimensional adaptive input-sampling mppt for thermoelectric energy harvesting. *IEEE Transactions on Circuits and Systems I: Regular Papers*, 66(12):4888–4900.

[Gould et al., 2008] Gould, C., Shammas, N., Grainger, S., and Taylor, I. (2008). A comprehensive review of thermoelectric technology, micro-electrical and power generation properties. In *2008 26th International Conference on Microelectronics*, pages 329–332. IEEE.

[Im et al., 2012] Im, J.-P., Wang, S.-W., Ryu, S.-T., and Cho, G.-H. (2012). A 40 mv transformer-reuse self-startup boost converter with mppt control for thermoelectric energy harvesting. *IEEE Journal of Solid-State Circuits*, 47(12):3055–3067.

[Liu and Zhao, 2020] Liu, H. and Zhao, C. (2020). Wearable electrochemical sensors for noninvasive monitoring of health-a perspective. *Current Opinion in Electrochemistry*.

[Nozariasbmarz et al., 2020] Nozariasbmarz, A., Collins, H., Dsouza, K., Polash, M. H., Hosseini, M., Hyland, M., Liu, J., Malhotra, A., Ortiz, F. M., Mohaddes, F., et al. (2020). Review of wearable thermoelectric energy harvesting: From body temperature to electronic systems.

[Radin et al., 2019] Radin, R. L., Sawan, M., Galup-Montoro, C., and Schneider, M. C. (2019). A 7.5-mv-input boost converter for thermal energy harvesting with 11-mv self-startup. *IEEE Transactions on Circuits and Systems II: Express Briefs*, 67(8):1379–1383.

[Romani et al., 2015] Romani, A., Camarda, A., Baldazzi, A., and Tartagni, M. (2015). A micropower energy harvesting circuit with piezoelectric transformer-based ultra-low voltage start-up. In *2015 IEEE/ACM International Symposium on Low Power Electronics and Design (ISLPED)*, pages 279–284. IEEE.

[Sze et al., 2008] Sze, N.-M., Su, F., Lam, Y.-H., Ki, W.-H., and Tsui, C.-Y. (2008). Integrated single-inductor dual-input dual-output boost converter for energy harvesting applications. In *2008 IEEE International Symposium on Circuits and Systems*, pages 2218–2221. IEEE.